Gabriel Pires de Souza

Licenciatura em Engenharia de Micro e Nanotecnologias

2D Nanostructures of V_2O_5 for energy storage devices

Dissertação para Obtenção do Grau de Mestre em
Engenharia de Micro e Nanotecnologias

Orientador: Volodymyr Khranovskyy, Professor Auxiliar, Linköping University, Sweden

Co-orientadores: Luís Miguel Nunes Pereira, Professor Associado, Faculdade de Ciências e Tecnologia da Universidade Nova de Lisboa, Portugal

Silvia Bodoardo, Professore Associato, Dipartimento Scienza Applicata e Tecnologia, Politecnico di Torino

Júri

Presidente: Prof. Doutor Rodrigo Ferrão, de Paiva Martins, Professor Catedrático do Departamento de Ciência dos Materiais da Faculdade de Ciências e Tecnologia da Universidade Nova de Lisboa

Arguentes: Dr. Ana Catarina Bernardino Baptista, Investigadora no CENIMAT/I3N, Faculdade de Ciências e Tecnologia da Universidade Nova de Lisboa

Vogais: Dr. Volodymyr Khranovskyy, Professor Auxiliar, Linköping University, Sweden

FACULDADE DE CIÊNCIAS E TECNOLOGIA
UNIVERSIDADE NOVA DE LISBOA

2D Nanostructures of V_2O_5 for energy storage devices

2D Nanostructures of V_2O_5 for energy storage devices

À minha mãe.

"Listen to me. I know that new situations can be intimidating. You're looking around and it's all scary and different. But you know, meeting them head on, charging right into them like a bull, that's how we grow as people."

Rick Sanchez

Agradecimentos

Independentemente, não poderia começar de outra forma os agradecimentos. À minha mãe, que depois de tantos anos a lutar para que eu tivesse tudo que podia querer para evoluir como pessoa, não me verá completar este percurso da vida. A ti, não há outra coisa sem ser um eterno agradecimento por teres existido, sem ti, nada disso teria sido possível. É com muita tristeza que acabo isso sem ti. Por isso, todos os agradecimentos são teus.

Também a minha avó, que sempre desempenhou um papel fundamental no meu crescimento. Nos últimos anos a vida não tem sido muito fácil connosco, foram muitas batalhas, vencidas e perdidas. Quero te dar o que eu sei que será a sua maior alegria, sou engenheiro. Eu consegui, e foi graças a ti.

Voltando ao protocolo, um especial agradecimento ao meu co-orientador, Prof. Luis Pereira. Durante muitos anos o professor me aturou, ajudou e ensinou. Tenho enorme alegria ao ter sido chamado de "o melhor aluno de micro 2". Obrigado por tudo, por ter proposto esse meu tema, pela sabedoria, e pela ajuda com Turim!

Ao meu orientador, Vlad, que apesar dos nossos altos e baixos durante a tese, acreditou que eu conseguiria atingir todos os objetivos propostos.

Aos professores Pedro Barquinha, João Paulo Borges, Isabel Ferreira e Hugo Águas, por nos momentos difíceis me ajudarem a concluir o curso.

A todos do Politécnico de Turim, Professora Dra. Silvia Bodoardo, Daniele Versaci, Ali. Vocês deram um produto à esta tese e me permitiram aprender muito sobre baterias.

Daniela, obrigado por todas as sessões de SEM improvisadas, além de produtivas eram sempre divertidas!

Seria impossível não ter nos agradecimentos o Professor Dr. Rodrigo Martins e a Professora Dra. Elvira Fortunato. Vocês são o combustível e o motor que permite uma geração de engenheiros continuar seguindo o caminho das Micro e Nanotecnologias, e a mostrar que é possível ser grande em Portugal.

Ao meu pai, que desde pequeno me fez perceber que vale a pena seguir os sonhos, por mais que pareça incompreensível ou errado para os outros. Que me dá suporte sempre que preciso. Acho que se você não tivesse se mudado para Portugal eu hoje não estaria aqui!

Minha querida priminha, Renata. Mala. Obrigado, não sei mesmo como que você me aguentou! Somos quase irmãos desde pequenos! Apesar da distância tenho certeza que continuamos muito unidos.

Aos meus tios Celeste e Luís, que sempre foram para mim os meus segundos pais.

Meus *prosts*, Danillo, Lucas e Otacílio. Vocês são o inicio de tudo! Minha infância, adolescência e agora a fase adulta… não há como não ter vocês em cada capítulo da minha vida. Meus irmãos, obrigado por todos os momentos de risadas, aventuras e muito FIFA! Sei que posso contar com vocês em qualquer momento, menos com o Otacilio que deve ter alguma festa de intercâmbio por aí.

Estenhaguens, que amizade improvável! Pedro, foi um enorme acaso termos nos conhecido e nos tornado tão amigos. Abriste a porta da tua casa e me deste uma nova família. Cláudia, Ronald e Maria, obrigado!

Pedro Mourão, feio… Quem diria hein? Já estamos crescidos e engenheiros! Obrigado por todas as conversas e todo o apoio! Tia Beatriz, não posso me esquecer de você! Um muito obrigado! Apesar de eu não falar muito por mensagens, eu não esqueço de vocês!

Ledo, Simões, Gonçalo, Zé! Meus grandes amigos desde a época de secundário! Tantas bebedeiras que tivemos juntos, tantos desabafos e conversas! Vir para Portugal foi muito fácil tendo vocês como amigos.

Madalena, estamos a tão pouco tempo juntos e já dividiste tantos momentos da minha vida comigo… Dás-me força, carinho, companheirismo… ralhas comigo quando preciso e me faz enxergar as coisas de outra maneira. Tenho muita sorte em ter você ao meu lado. Muito obrigado!

Agora a faculdade… Titó, se não tivesses aceitado a ideia parva de fazer 7 cadeiras todos os semestres não estávamos aqui. A nossa competição constante resultou! Passaste de amigo, para irmão e cunhado, obrigado! Macedo… sem ti o curso não tinha brilho! Obrigado por várias cadeiras que me fizeste e por todas as risadas que demos. Wubba Lubba Dub Dub!!!! Bruninho, gato… desde o primeiro dia de faculdade, naquela casa de banho de física… houve e ainda há muito amor entre nós! Tu espalhas magia amigo! Obrigado! SACANITAAAA! Um curso não se faz sozinho! Graças a ter que te explicar 50x as matérias, meu curso foi mais fácil! Miga Ana, como que eu passei tantos anos da faculdade sem te conhecer? Foste fundamental nesta reta final. Conseguiste me levar pra má vida!

Dandan e Pinto, a completarem meus ‘Pussies’ favoritos! Não sei ao certo quando nossa amizade começou, mas essas são as melhores. Simplesmente aconteceu e a faculdade foi melhor graças a vocês.

Ribancelli, Farinha, Chamiço, foram tantos fritanços a estudar na 202 que no final foram mais divertidos do que outra coisa. Obrigado por esses momentos.

Raquel ‘Coisa’ Barras… Foi todo o teu apoio e ajuda durante a época da tese que se calhar devias ter uma seção nesta tese só pra ti. Sem você essa tese com certeza não estaria feita… Muito obrigado mesmo teacher!

A todos os meus companheiros dos últimos tempos, com uma menção honrosa ao meu amigo Gil ‘Trigo’ Dias, que conviveram comigo diariamente seja no Open Space ou nos laboratórios do CENIMAT, alunos e investigadores, toda essa experiência foi muito melhor graças ao ótimo ambiente que é o CENIMAT.

Resumo

Hoje em dia vivemos num mundo sem fios, conectados a todos. Nossos telemóveis, computadores e até nossos eletrodomésticos, como relógios e câmaras estão utilizando de baterias como a sua forma principal de alimentação. Cada dia mais se torna mais complexo sustentar um aumento da demanda do consumo de energia, enquanto tenta se manter uma boa capacidade de bateria. Assim, devemos desenvolver baterias ainda mais baratas, mais eficientes e até menores do que nunca.

Muitos tipos de baterias foram desenvolvidos no passado, como baterias de níquel e enxofre, porém são as baterias de lítio que tiveram as melhores melhorias, graças a sua alta estabilidade e facilidade de produção. Há vários métodos de melhoria numa bateria de lítio, e um dos mais eficientes é a melhoria no cátodo. Para este trabalho, Pentóxido de Vanádio, um material abundante na terra, barato e com uma densidade de energia melhor que os materiais tradicionais, foi utilizado.

Exfoliação em fase líquida foi o método utilizado para a obtenção das nanoestruturas, enquanto DRX, SEM, BET e XPS foram utilizados para confirmar a sua estrutura. Para as baterias, testes galvanotáticos de carga e descarga e voltometria cíclica foram utilizados para testar a performance deste material como cátodo.

Palavras-chave: Vanádio, Pentoxido de Vanádio, Cátodo, Nanoplates, Baterias de iões de lítio, Exfoliação em fase líquida

Abstract

Nowadays we're living in a wireless connected world. Our phones, computers, and even everyday appliances such as clocks, cameras, etc. are getting out of the grid using batteries as its main source of energy. It's becoming more and more demanding to sustain an increase in energy consumption of these devices while maintaining a good battery life. As a result, we must develop batteries that are cheaper, better and smaller than ever before.

Many batteries have been developed in the past few years, such as Nickel and sulfur batteries. But it is the lithium-ion batteries that has the most significant improve in use, due to its high stability and easiness to produce. There are plenty of ways to improve a Lithium-ion battery, and the most effective and useful is improving the cathode. For this, Nanostructured Vanadium Pentoxide, an earth rich, cheap and with higher energy density than traditional materials was used in this present work.

Liquid-phase exfoliation was used to produce the nanostructure, while XRD, SEM, BET and XPS were used to confirm its structure. For the batteries, galvanostatic charge-discharge and cyclic voltammetry were used to test its performance as a cathode material.

Keywords: Vanadium, Vanadium Pentoxide, Cathode, Nanoplates, Lithium Batteries, Liquid-phase Exfoliation

Index

Figure Index

Abbreviations

2D – Two-dimensional
BET – Brunauer–Emmett–Teller
CV – Cyclic Voltammetry
DMC – Dimethyl carbonate
EC – Ethylene carbonate
FESEM – Field Emission Scanning Electron Microscope
HT-XRD – High Temperature X-ray Diffraction
JCPDS – Joint Committee on Powder Diffraction and Standards
K-Ion – Potassium Ion
Li-ion – Lithium ion
LIB – Lithium ion battery
$LiPF_6$ – Lithium hexafluorophosphate
$NH_4V_3O_8$ – Ammonium Trivanadate
NMP – N-methyl-pirrolidone
SEM – Scanning Electron Microscope
V_2O_5 – Vanadium Pentoxide
XPS – X-ray photoelectron spectroscopy
XRD – X-ray Diffraction

1 Introduction

Two-dimensional (2D) materials have attracted great interest after the discovery of graphene, due to their structural anisotropy and enhanced properties compared to raw material[1]. Vanadium pentoxide (V_2O_5) is a cheap, earth-rich, layered material with high theoretical capacity, making it a suitable candidate to produce nanosheets and to be a cathode material for Lithium Ion Batteries (LIBs). Based on this, exfoliated V_2O_5 nanoplates were developed, characterized and tested as a cathode for Li-ion batteries.

1.1 2D Nanomaterials

Graphene started the interest for 2D materials in 2004, and can now be used in a wide range of applications, from energy conversion and storage systems, to electronic and optical devices [2,3] . Nonetheless, while being such a novel material, since is composed of only carbon, this characteristic cap its versatility, either by composition or structural [1].

As a result, the research for alternative 2D materials became a topic of great interest [4]. These materials have strong in-plane bonds while having weak Van der Waals interactions between layers, thus to get nanosheets those interactions should be disrupted[5]. Ideally, materials that are exfoliated into ultrathin nanosheets have all atoms exposed to the surface, making the surface phase of the material one important feature to analize[1]. Given the unique 2D structure, properties such as electrical conductivity, photonics, magnetics, etc. - compared to bulk counterparts -, open new characteristics to transistors, sensors, supercapacitors and batteries [6]. In ultrathin 2D nanomaterials, the electron confinement in the two dimensions of the material without interlayer interactions enhances electronic properties. Also, the atomic thickness provides excellent mechanical flexibility and optical transparency, making them suitable for optoelectronic devices. Likewise, its large lateral size and thin thickness gives these materials high surface area, which greatly improves lithium ion batteries [7].

1.1.1 Exfoliation of Layered Materials

To get the full potential of these promising materials, it is necessary to develop a reliable, facile, feasible and reproducible method to get thinnest possible nanosheets. Many methods have been studied and developed, such as mechanical cleavage [9], liquid-exfoliation [10], ion-intercalation and exfoliation [11], chemical vapor deposition [12], etc.. These methods can then be classified as: top-down or bottom-up.

The top-down method consists on the direct exfoliation of layered bulk materials into 2D structures as thin as single-layer, in which several forces are used to break the weak Van der Waals links between layers. In other hand, bottom-up relies on direct synthesis of 2D materials from different precursors via chemical reactions.

1.1.2 Synthesis of 2D Nanomaterials via Liquid Exfoliation

Liquid-phase exfoliation is one among many techniques to produce 2D ultrathin nanosheets from layered bulk materials. This method usually has high yield, does not require high-cost techniques such as vacuum-drying or high temperature and pressures as solvothermal synthesis [13].

Nanosheets are obtained based on the principle that the precursor powder (i.e. V_2O_5) is immersed in a solvent that intercalates between the interlayer space, which causes a swelling in the material, weakening the interaction between layers, opening space for a mechanical stress disrupt the layers, i.e. sonication, creating nanosheets [14] (Fig. 1). Although the sonication can break the Van der Waals force between the sheets, it cannot break the covalent bonding existing in each layer.

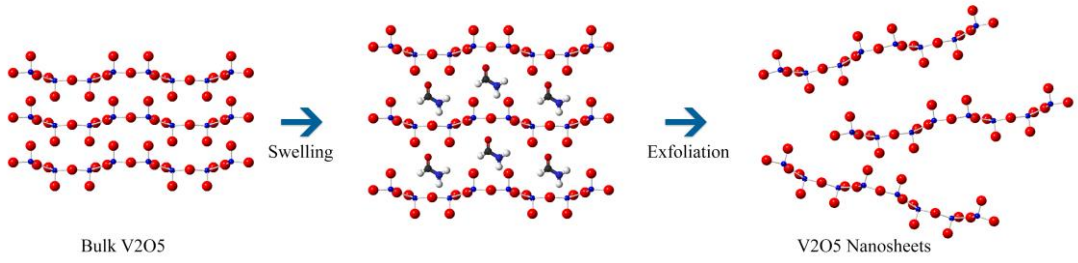

Fig. 1 - Exfoliation process of V_2O_5 via liquid-phase exfoliation using formamide as solvent

The choice of the solvent is a key factor in a good exfoliation process, as with a good matching surface tension between the solvent and the layered crystal minimizes the energy and increases the efficiency of the process, also, it helps stabilizing the exfoliated nanosheets and avoiding their restacking and aggregation [7].

1.2 V_2O_5 – Structure and Applications

Vanadium is a useful transition metal as it is earth-rich, cheap and has plenty uses in scientific and industrial areas, due to several different oxidation states, ranging from +2 to +5 [15–17]. As a result, Vanadium compounds have been widely studied for applications such as optoelectronic [18], sensors [19] and energy storage [20].

Specifically, V_2O_5 has a crystal structure formed by stacking layers, perpendicular to c-axis via Van der Waals interactions [21]. This layered structure makes V_2O_5 (Fig. 2) a promising candidate for LIBs, as it allows reversible ions intercalation, which makes them suitable for electrochemical energy conversion and storage [16].

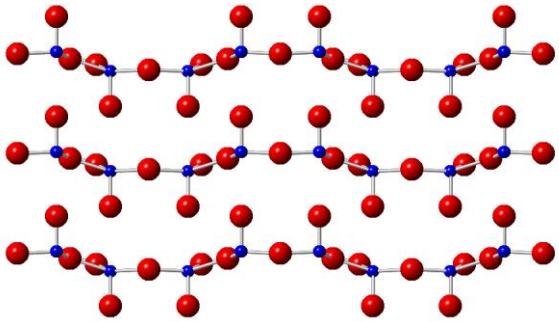

Fig. 2 – Representation of Orthorhombic V_2O_5 (Pmnm) layered structure

Not only that, but V_2O_5 also has a high theoretical capacity of 294mAh g^{-1}, thanks to its 2 Li^+ intercalation/deintercalation per unit formula (Eq. 1), which is higher than most commonly used cathode materials, such as $LiCoO_2$ (140mAh g^{-1}), $LiMn_2O_4$ (148mAh g^{-1}) and $LiFePO_4$ (170mAh g^{-1}) [22,23].

$$V_2O_5 + xLi^+ + xe^{-1} \leftrightarrow Li_xV_2O_5 \quad (1)$$

Despite many advantages, V_2O_5 has some downsides due its poor structural stability during intercalation-deintercalation process, poor kinetics due to low diffusion coefficient of lithium ions, and low electric conductivity [24–26].

As mentioned earlier, nanostructured materials can significantly improve some features from a material, and with this, many nanostructures for V_2O_5 have been proposed, such as nanorods [27,28], nanosheets [29,30] and three-dimensional nanoflowers [31], which significantly improved V_2O_5 to be used as electrode material. However, 2D materials, such as nanosheets or nanoplates, seems to be the most valuable structure, because of unique planar configurations that offers shortened diffusion path for lithium ions and more active sites [24,32,33].

1.3 Lithium-ion Batteries

By definition, a battery is a device capable of converting chemical potential into electric energy, through chemical reactions [34]. Researchers have been developing various kinds of devices to reduce or consumption of fossil energy [35,36], and one of the most researched topic is lithium-ion batteries.

Japanese company Sony kicked off the manufacturing of Li^+ batteries in 1991, although initial research on this topic was conducted by Armand in the late 70s [37], when trying to use intercalation materials with different potential for the electrodes [38]. This is the same working principle used until nowadays in newer lithium ion batteries. As shown in Fig. 3, the working principle consist in an anode (source of lithium ions) with a cathode (sink for lithium ions) having different potential so lithium ions can flow through a medium that provides pure ionic conductivity, the electrolyte [39].

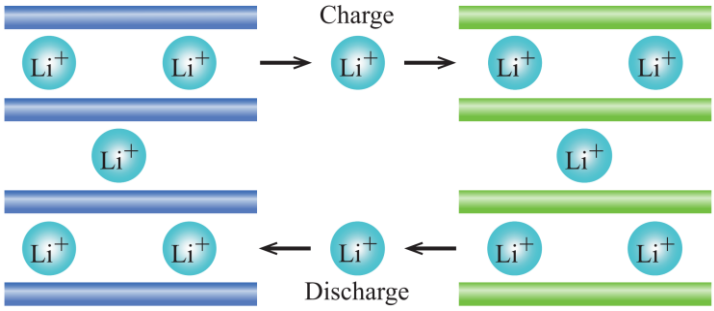

Fig. 3 – Simplified working principle of a Lithium Ion battery

During charging and discharging, electrons travel through the external circuit from the anode to the cathode. At the same time, Li+ ions travel between the two electrodes through the electrolyte, in the same direction as the electrons. This flow enables the conversion of chemical energy into electrical energy, and thus the storage of electrochemical energy within the battery [40].

There are three main factors that can be considered the most important ones to improve a lithium-ion battery (LIB): rate capability, cyclability and power density [41]. A promising, and effective, method to improve these factors is the design of nanoscale electrode materials, as they are an effective method to shorten the Li^+ diffusion distance during the charge-discharge process, as well increasing the interfacial contact area between the electrode and electrolyte, enhancing both specific power density and energy density [42]. As said earlier, 2D nanoarchitectures can improve lithium storage, as it has large exposed surface area, and shortened ion diffusion path, offering more lithium-insertion channels [32].

1.3.1 Button Cell Battery

This type of batteries is mounted together as a single cell, varying its size, usually 5 to 25 mm in diameter, according to the application. Given its small size, their usage is mainly for low electrical power devices, such as toys, watches, calculators or portable devices, and to power memory backup for electronic devices, i.e. motherboard [43]. Coin cell, a type of button cell, is commonly used in laboratories to test the capacities and rate capabilities of new materials as they are developed [44].

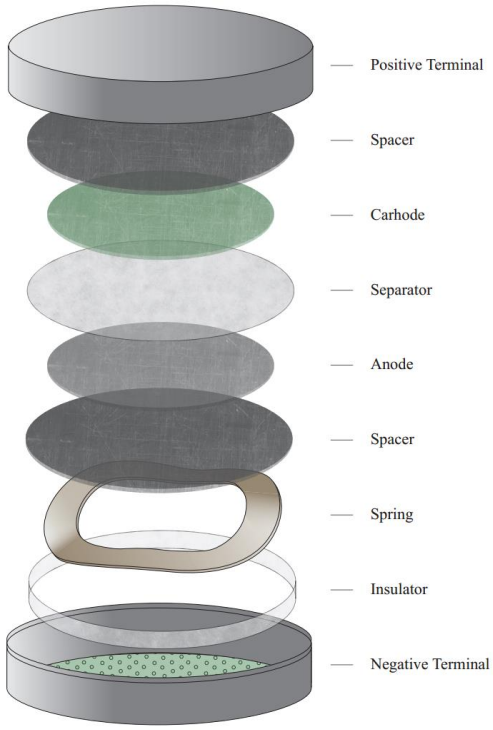

Fig. 4 - Typical button cell (coin cell) montage

These battery components are mounted inside a metal housing, designed by a lower conductive can and a top conductive lid. Inside, both electrodes are usually separated by a porous separator, and the electrolyte exists within pores of the separator [45,46]. To increase conductivity between electrodes and housing, a spacer can be used [44]. Fig. 4, shows a typical coin cell structure as used in this present work.

This dissertation aims to produce nanostructured V_2O_5 via liquid-exfoliation, a simple, effective and high-yield method of production, and use those nanoparticles to create a high-performance Li^+ battery. Morphological characterization and electrochemical performance were studied for a direct comparison with bulk V_2O_5. Additionally, working coin-cells with both materials were successfully made and tested.

1.4 State-of-the-art on V_2O_5 batteries

As shown by An et al. [30], ultrathin V_2O_5 nanosheets were obtained with high rate capability for lithium batteries. The nanosheets were prepared through supercritical solvothermal reaction followed by annealing treatment. The ultrathin V2O5 nanosheets exhibited a capacity of 108 mAh g^{-1} at 10C and 146 mAh g^{-1} at 1C, and beyond that, they had excellent cyclability with little capacity loss after 200 cycles at 10C, corresponding to 96% of its initial capacity.

Another example of remarkable ultrathin V_2O_5 nanosheets cathodes was shown by Rui et al. [22], where few-layer V_2O_5 nanosheets with thickness of 2.1-3-8nm were successfully synthesized via the same technique described in this present work, liquid-phase exfoliation. The as-obtained V_2O_5 nanosheets were tested for their lithium storage performance as a cathode material and the results were interesting, such as 292 mAh g^{-1} for the first discharge capacity. Their tests were performed at a much lower C-rate compared to An et al., at 0.5C, but their results are nonetheless remarkable, with a charge retention of 93.8%.

These works show us how promising Vanadium Pentoxide can be, specially if combined with 2D nanostructure, enhancing both capacity and stability of lithium-ion batteries, *ergo*, being a potential candidate to be used as a cathode. These ultrathin nanosheets shows great cycling stability, high Coulombic Efficiency and reversible capacity, and can ally fast-charging and high-power deliver.

2 Experimental Section

2.1 Production method

2.1.1 Synthesis of V_2O_5 nanostructure

The synthesis of V_2O_5 nanostructures was based on liquid exfoliation method [47], with few modifications that allowed the reduction of process time, i.e. bath sonication. Analytical grade V_2O_5 (Sigma-Aldrich, 98%) was dispersed in Formamide (Sigma-Aldrich) in a proportion of 1:2 and left under vigorous stirring for 24 hours until a brown paste was formed. Afterward, the resulting paste was left under bath sonication (BANDELIN Sonorex) for 3h. To isolate the V_2O_5 nanostructures, the subsequent material was washed by centrifugation (Thermo Scientific Multifuge X1R) at 6000rpm, in ethanol (Sigma-Aldrich, 99.8%), several times (usually 5 times) on a Falcon tube (50ml). This step created an intermediate state of $NH_4V_3O_8$. Then, the material was dried on a hot plate, in air, at 60º C for 2h. To further eliminate the intermediate state, the material was later quick heated on a hot plate at 400º until the color changes from orange to bright orange, which occurs in few seconds.

2.1.2 Battery fabrication

2.1.2.1 Slurry preparation

Two slurries were produced, one containing raw V_2O_5 (Sigma-Aldrich, 99%) and another containing the as-obtained nanostructured V_2O_5. Both were made following the 70:20:10 ratio (Active Material : Conductive Agent : Binder). 0.05g of PVdF were dissolved under stirring in 0.5ml of NMP. In the meantime, 0.35g of V_2O_5 and 0.1g of C65 were mixed in a mortar, in order to make it more uniform. After complete dissolution of PVdF, the as-obtained powder of V_2O_5 + C65 was added to the solution. 1.5ml of NMP were added to obtain the desired thickness of the slurry. Slurry was left under stirring overnight to obtain a homogeneous solution (Appendix Fig. A. 1.)

2.1.2.2 Cathode preparation

To fabricate the cathode, the resulting mixture was shear casted onto aluminum foil, at the speed of 50mm s^{-1}, with a 300µm thick blade, then left to dry at room temperature overnight. It was later punched into small disks (Ø=16mm) for coin cell, and smaller disks (Ø=10mm) for T-cell. After fully dried, the sheet was pressed under high load (150 bar). Further drying in vacuum at 120º C for 4h.

2.1.2.3 Battery fabrication

Both coin cell and T-cell (Appendix Fig. A. 2) batteries were assembled in an argon-filled glove-box (M3Braun UNIlab sp), where both moisture and oxygen levels were less than 1ppm. In both cells, lithium foils were used as anode, $LiPF_6$ 1M in ethylene carbonate (EC)/dimethyl carbonate (DMC) (1/1, v/v) + 1% VC (Vinylene Carbonate) was used as electrolyte and double-layer Whatmann paper was used as separator. The assembled battery was taken out of the argon glove-box to be compressed in a dry-room with humidity less than 5% and, therefore, sealed.

2.2 Characterization Methods

2.2.1 V_2O_5 Characterization

2.2.1.1 XRD

Samples of raw and nanostructured V_2O_5 were characterized by XRD with a PANalytical X'Pert PRO diffractometer equipped with a X'Celerator detector and using CuKa radiation. The diffraction patterns were collected in Bragg-Brentano configuration in 2θ, ranging from 5º to 65º with a 0.02º step size. Both samples were compared with the experimental XRD patterns to standards compiled by JCPDS, and then compared to each other.

2.2.1.2 HT-XRD

Nanostructured V_2O_5 was further studied with HT-XRD (PANalytical X'Pert PRO) under air to understand when the transition of $NH_4V_3O_8$ to V_2O_5 occurs. The V_2O_5 powder was placed on a platinum strip, and the patterns were acquired between 30ºC and 500ºC with a step of 50ºC.

2.2.1.3 SEM

SEM (Carl Zeiss, Auriga) was used to observe the microstructure of the synthesized V_2O_5 nanostructures, as well the raw material. Powders were spread on a double-face carbon tape without any treatment. Images were analyzed with the software ImageJ to study the dimensions (thickness and diameter) of the V_2O_5 nanostructures.

FESEM Zeiss Supra™ 40 was used to further study the thickness of the nanostructured V_2O_5, at Electrochemical Department - Politecnico di Torino

2.2.1.4 TG-DSC

Evaporation of NH_4^+ from the sample was verified with DSC at air temperature varying the temperature from 25º to 400ºC. The loss of mass shows the optimal temperature to transform the intermediate state into pure V_2O_5

2.2.1.5 XPS

The XPS measurements were carried out with a PHI Model 5800 (USA) electron spectrometer, at Politecnico di Torino, equipped with an Aluminum anode (1486 eV) monochromatic source with a power of 25.6 W and the high-resolution scan with a 11.75 eV pass energy. The instrument typically operates at pressures below $5x10^{-8}$ mbar. A PHI patented dual beam charge neutralization method, combining low energy ions and electrons, was employed to reduce the possible charging effect of the X-rays on the samples.

2.2.2 Battery Characterization

2.2.2.1 Galvanostatic Charge and Discharge

To study the electrochemical characteristics of the materials, an ARBIN multi-channel battery test system with galvanostatic charge and discharge in the voltage range of 4.0-2.0 V was used. This allows to study the specific capacity, coulombic efficiency and cycling performance.

2.2.2.2 Cyclic Voltammetry

CV was used to study and understand the redox reactions occurring in the material. Tests were performed in a T-cell battery, using three electrode configuration (Lithium was the reference electrode), with CH Instruments CHI660D, in the range of 2-4V, and a scan rate of $1mVs^{-1}$.

3 Results and Discussion

Herein is discussed the synthesis of V_2O_5 nanostructure by liquid-exfoliation and the production of a functional cathode for Li^+ batteries.

3.1 Liquid-exfoliation of V_2O_5

Initially many techniques were employed to exfoliate V_2O_5 into nanosheets, such as solvothermal, hydrothermal and sol-gel, but after many attempts the most successful was liquid-exfoliation due its simplicity, quickness and efficiency. Parameters such as solvent, solvent ratio and sonication time were studied on a trial and error basis.

3.1.1 Influence of solvent

Based on the work of Nicolosi et al. [47] and Rui et al. [7], two solvents were chosen due to its efficiency and availability at the lab, N-methyl-pirrolidone (NMP) and Formamide. Both solutions were carried in the condition showed in Chapter 2.1.1, for 3h sonication only, and the best solvent was chosen by direct analysis of SEM images shown in Fig. 5.

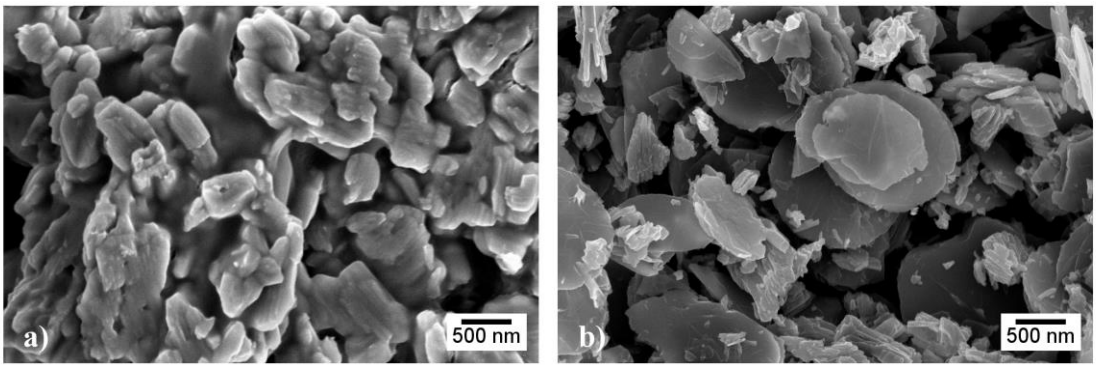

Fig. 5 - SEM images of a) V_2O_5 structure dispersed in NMP, and b) V_2O_5 nanostructure dispersed in Formamide

Resultant product of liquid-exfoliation of NMP is much more aggregated than the one in Formamide. With the later, the result is a plate-shaped, very thin (around 20~60nm) particle. Moreover, few more experiments were performed under the same condition to attest its reproducibility and while the product of Formamide exfoliation maintained consistent results, the one with NMP varied along the experiments. For these reasons, liquid-exfoliation of V_2O_5 with Formamide was preferred.

3.1.2 Influence of solvent ratio

It was initially thought that with the increase of solvent ratio more exfoliated the sheets could be, as it would increase the concentration of Formamide molecules inside the sheets of V_2O_5 to help disrupt weak Van der Waals forces with sonication. Three ratios were tested - 1:1, 1:2 and 1:5 - and surprisingly 1:1 and 1:5 produced almost the same particles' morphology, while 1:2 shows exceptionally thin nanoplates with large lateral size, as observed in Fig. 6.

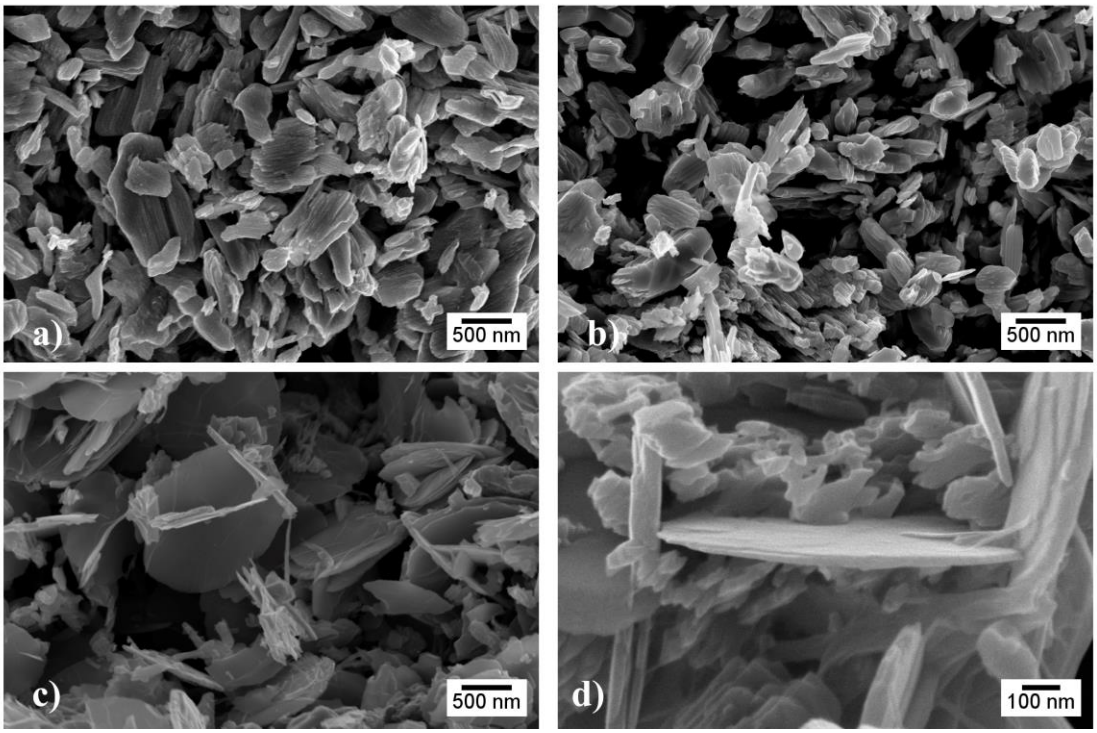

Fig. 6 – SEM images of different ratios, a) Ratio of 1:1, b) ratio of 1:5, c) 1:2 and d) close-up of one nanoplate of V_2O_5 (3 hours sonication) with circa 30nm thick

No ratios could produce uniform plates while maintaining a high yield. Despite that, a ratio of 1:2 was the only that could produce nanoplate like structures, despite not being homogeneous along the entire sample. As shown in Fig. 6 c) and d), it's clear to see that nanoplates are present, but also some particles like the ones in Fig. 6 a) and b). One hypothesis for this is the bulk V_2O_5 didn't have enough time to exfoliate, or the solvent couldn't penetrate well enough between the interlayer space, therefore creating just broken pieces of bulk V_2O_5.

3.1.3 Influence of Sonication Time

Sonication time is one important parameter, as if not long enough, will not result in large quantities of exfoliated material, while if left too much, could result in broken pieces of layered material. With our bath sonicator, we cannot control the frequency or intensity of the waves, and are also unknown, so the time is the only parameter we can control in this process. For this study four times were chosen, 3h, 6h, 12h and 24h. Four individual samples were prepared following the same method as before.

The result for 3 hours sonication is shown before in Fig. 6 c) and d) demonstrating a good ratio between nanoplate obtainment and broken-down pieces of V_2O_5. But with the increase of sonication time, the less this ratio is, demonstrating that is not worth to leave the solution for an extended period of time.

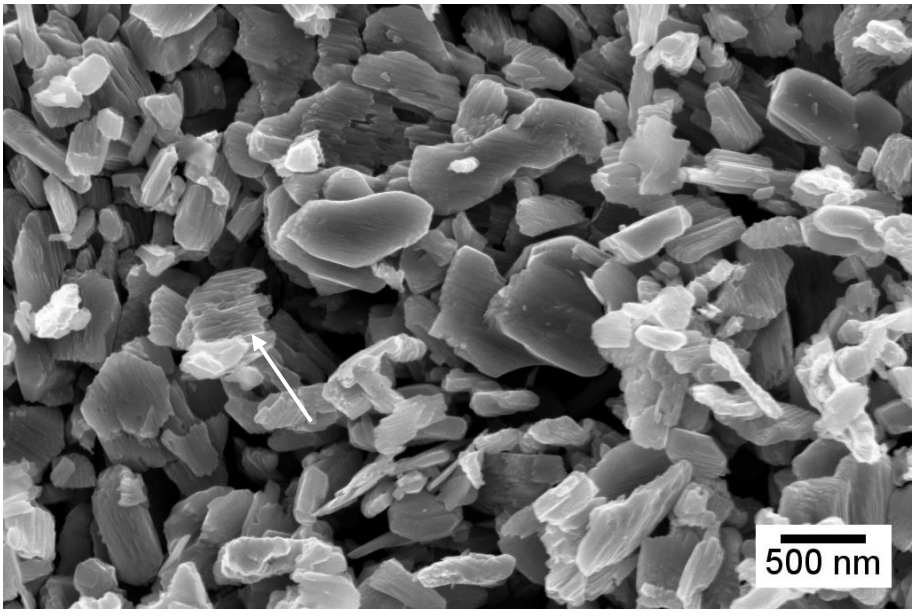

Fig. 7 - V_2O_5 nanoparticles after 6 hours of sonication

In Fig. 7 we can observe that resultant particles are quite similar as the one observed in Fig. 6 b), with many broken pieces of V_2O_5, with a surface that is not smooth. That could be linked to some aggregation of the material after its exfoliation, or the heat treatment to dissolve NH_4^+ melting some of the material.

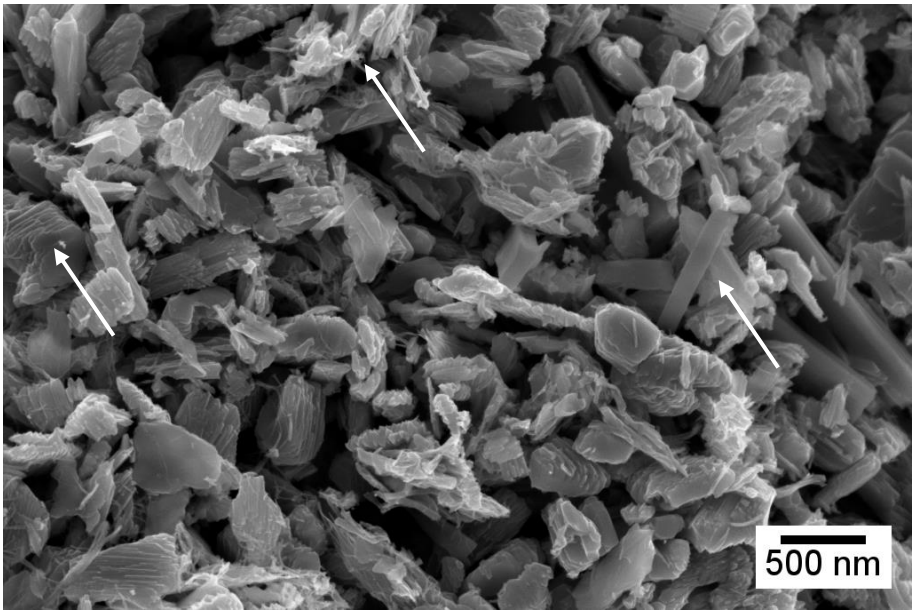

Fig. 8 - V_2O_5 nanoparticles after 12 hours of sonication

Increasing the time to 12 hours is possible to observe multiple different structures, with three of them shown in Fig. 8. We can see the re-stacking mentioned before, and the effect is more prominent and we can clearly deduce that there are many sheets of V_2O_5 sitting on top of each other. Also marked, are some tiny shapeless pieces, indicating that sheets were broken due to sonication. And last, it is present in this sample some sort of well-defined rod structure not present in any other sample.

Finally, after 24 hours of sonication (Fig. 9) the structure again shows the same re-stacking and the same shapeless pieces present in previous samples. But for this longer period of time is also possible to observe nanoplates amongst all the other pieces. Unfortunately, due to their position in the sample we could not estimate their thickness, but it seems consistent with the ones made with 3 hours of sonication.

So, after studying those four time periods, both 6 and 12 hours were discarded. The results from 3 and 24 hours were comparable at least, but since it is better and quicker to use only 3 hours, that was the chosen time for this present work.

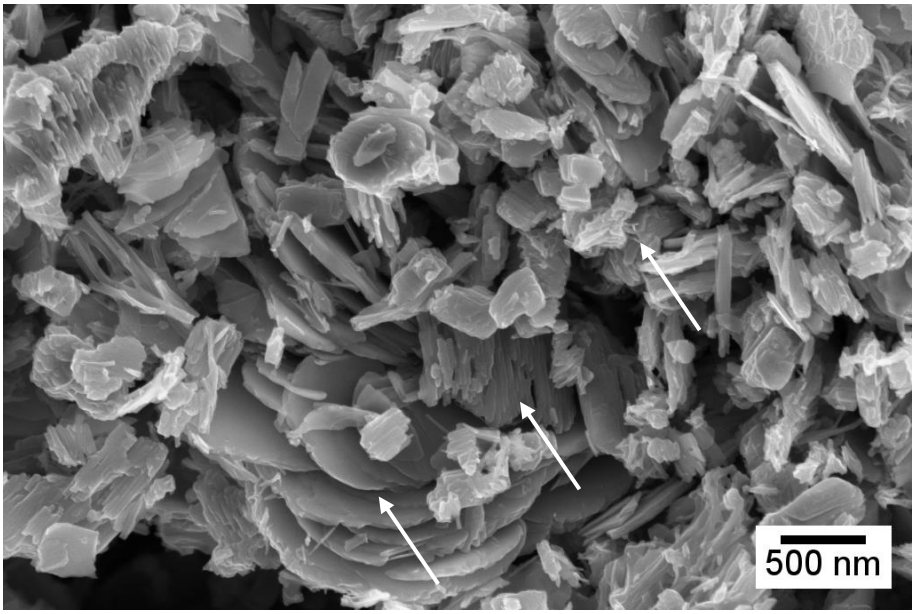

Fig. 9 - V2O5 nanoparticles after 24 hours of sonication

3.2 Morphological Characterization

Fig. 10 shows a before and after SEM image of bulk V_2O_5 that undergone liquid-exfoliation treatment. The dominant different is the decrease in size, proving the effectiveness of the used method. Also, an interesting detail is present in Fig. 10 - Direct comparison of liquid-exfoliation process, a) Bulk V_2O_5 and b) Nanoplates of V_2O_5, a nanoplate sits on-top of another, so thin that it is possible to see the plate that lies beneath.

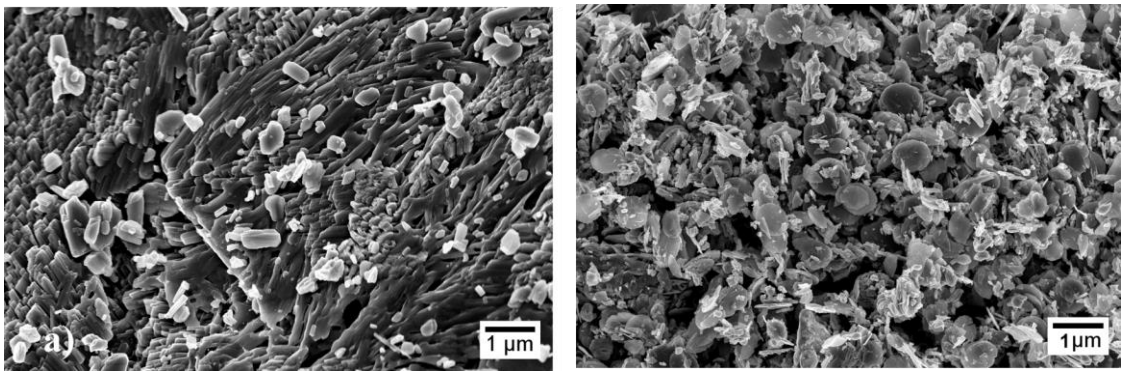

Fig. 10 - Direct comparison of liquid-exfoliation process, a) Bulk V_2O_5 and b) Nanoplates of V_2O_5

Another factor to consider is the difference in structure between the supernatant and the precipitate (Fig. 11). The supernatant shows a clear, uniform and well-defined disk shape, but the thickness is 10 times higher than the precipitate and the yield is extremely low. For this reason, the later was chosen to continue under tests.

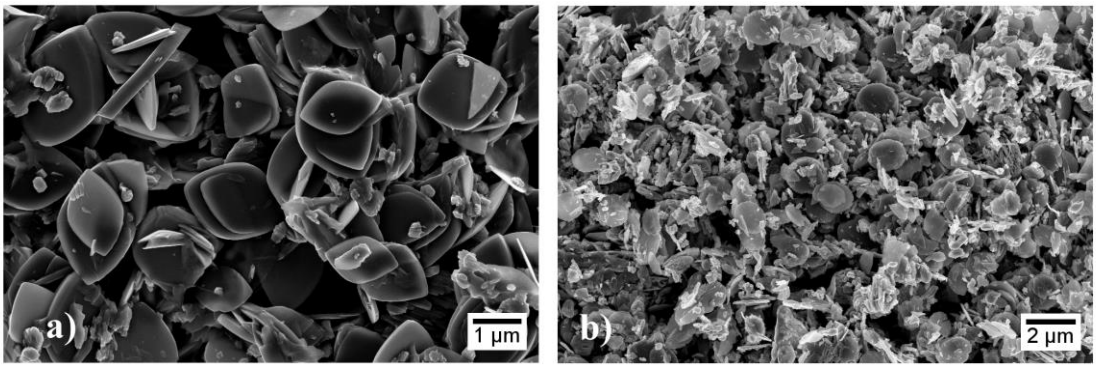

Fig. 11 – a) Supernatant sample after first washing in ethanol @ 6000rpm and b) precipitate collected after final washing

Since the procedure is done using a solvent, XRD analysis, as well XPS, was made to confirm that the final product was still pure V_2O_5. The result was not ideal, but to some extent expected, since one of intermediate state of V_2O_5 in this process is Ammonium Trivanadate ($NH_4V_3O_8$) and it was present in the sample (Fig. 12). Since Ammonium is an organic solvent, it was proposed that a simple thermal treatment with at least 70º C would be enough to evaporate it. This idea is supported by the work of Kaus-Jurgen et al. [48] with the thermal decomposition of Ammonium Metavanadate.

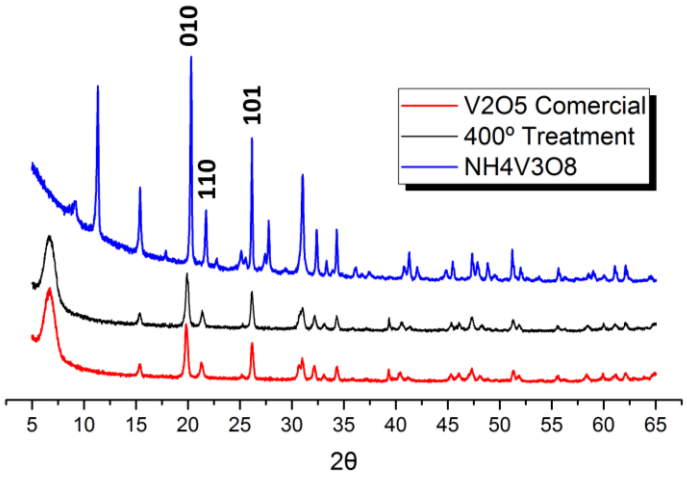

Fig. 12 -XRD patterns for samples of bulk V_2O_5 (red) $NH_4V_3O_8$ before thermal treatment (blue) and 2D nanostructured V_2O_5 (black)

To determine the best temperature for the thermal treatment, HT-XRD study, with the variation of temperature was made from 30º to 500º, and is possible to see the transition of the material between 300º and 400º. To complement this, TG-DSC study was performed to observe the exact temperature where a loss of mass occurs. With TG-DSC (Fig. 13) is possible to observe that 5.92% weight loss at 298º, indicating the evaporation of the solvent at said temperature. HT-XRD can be found at Fig. A. 3

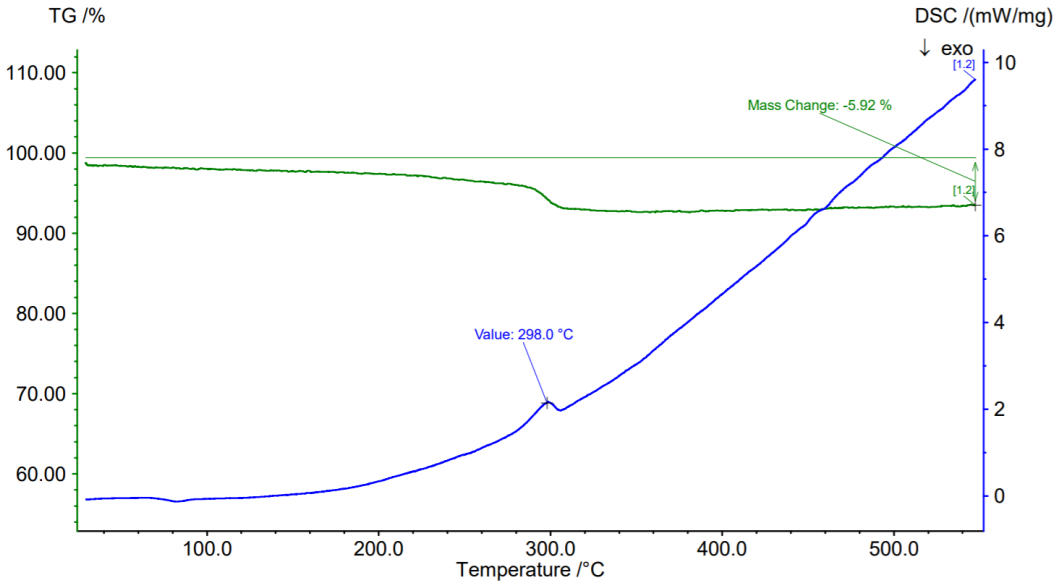

Fig. 13 - TG-DSC study on NH4V3O8 to determine temperature transition of the material

XPS study for the nanostructured V_2O_5 was made to investigate the chemical state, as shown in Fig. 14.The binding energies obtained in the XPS analysis were corrected for specimen charging by referencing the C_{1s} line to 284.6 eV. Core level binding energies of $V2p_{3/2}$ (Fig. 14 a)) can be divided in four main peaks, 515.61, 517.05, 523.06 and 524.64 eV. The first two peaks can be attributed to V^{5+} and V^{4+} species, respectively. The O1s spectrum is broad and asymmetric, divided in three peaks, indicating the existence of three different oxygen species. The peak located at 529.90 eV can be assigned as oxygen in V_2O_5. [49]

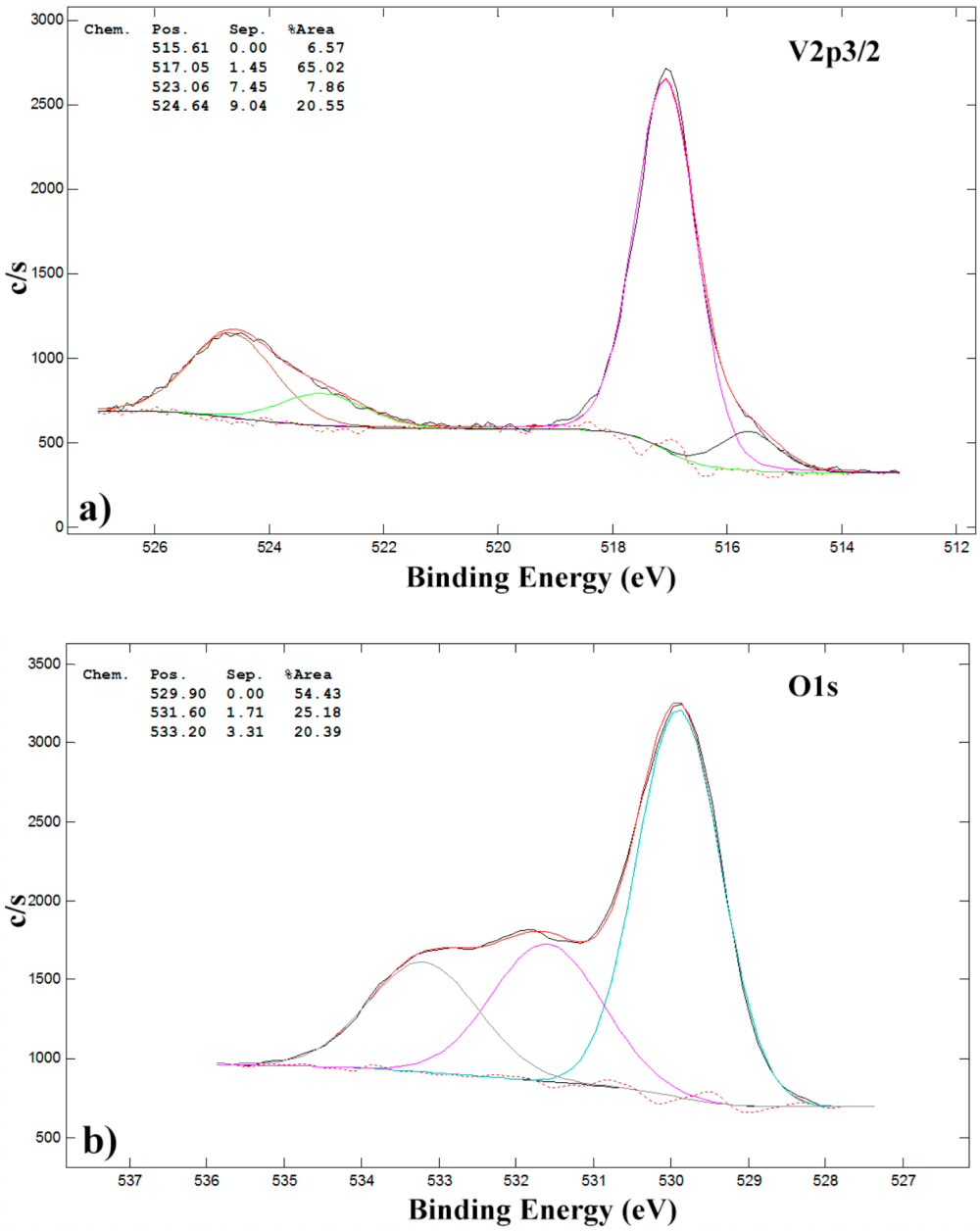

Fig. 14 XPS observation of the a) V2p3/2 spectrum and b) O1s spectrum

With the results of XRD confirming the successful production of 2D nanostructured V_2O_5 a FESEM study was performed to further study the thickness of the nanostructures. The results were quite interesting with some particles reaching the sub-20nm thickness, as seen in Fig. 15.

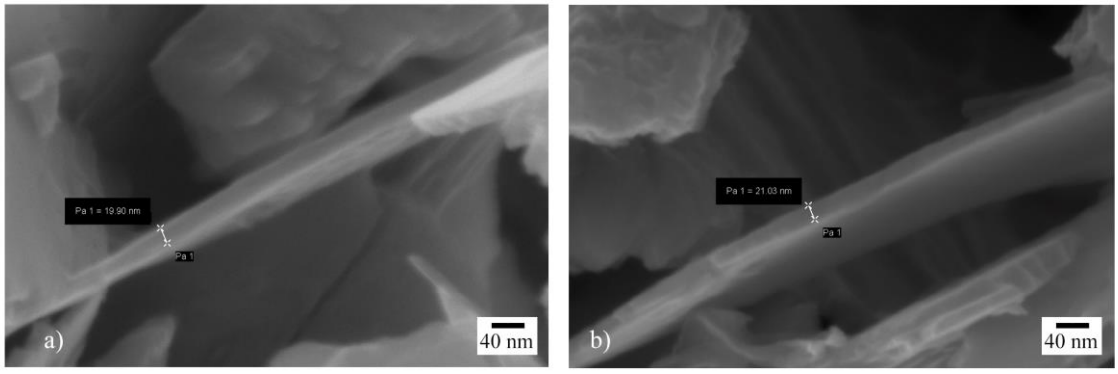

Fig. 15 – Zoomed images of V_2O_5 nanoplates with a) Nanoplate with 19.90nm and b) Nanoplate with 21.03nm

3.3 Electrochemical Performance

After determining the best parameters for the synthesis, V_2O_5 batteries were successfully made in this dissertation using Coin-cell and T-cell structure, the latter being used only for cyclic voltammetry (CV) due its three contacts configuration. Said batteries are depicted in Fig. A. 2. Electrochemical performance was evaluated using CV at scan rate of 0.1mV s^{-1} in a potential range of 2.0 to 4.0V. Charge/discharge technique and its cycling performance was tested using galvanostatic charge-discharge method.

3.3.1 Cyclic Voltammetry

Fig. 16 shows the first three CV cycles of Nanoplate V_2O_5 and Bulk V_2O_5. The redox peaks correspond to different oxidation (Positive currents) or reduction (negative currents) steps of Lithium in the structure of V_2O_5. Consequently, different amounts of Li^+ can be intercalated and deintercalated in V_2O_5. In Fig. 16 a) four main redox pairs were observed at around 3.63/3.6, 3.45/3.4, 3.34/3.2 and 2.49/2.3 V, which associates to the reversible lithium intercalation/deintercalation on V_2O_5 forming, respectively, α-$Li_xV_2O_5$, ε-$Li_xV_2O_5$, δ-$Li_xV_2O_5$ and γ-$Li_xV_2O_5$, expressed in the equations (2) - (5) [50]. The same principle applies for Fig. 16 b).

$$V_2O_5 + xLi^+ + xe^- \leftrightarrow \alpha Li_xV_2O_5 \ (x < 0.1) \quad (2)$$
$$V_2O_5 + xLi^+ + xe^- \leftrightarrow \varepsilon Li_xV_2O_5 \ (0.35 < x < 0.7) \quad (3)$$
$$V_2O_5 + xLi^+ + xe^- \leftrightarrow \delta Li_xV_2O_5 \ (0.9 < x < 1) \quad (4)$$
$$V_2O_5 + xLi^+ + xe^- \leftrightarrow \gamma Li_xV_2O_5 \ (1 < x < 2) \quad (5)$$

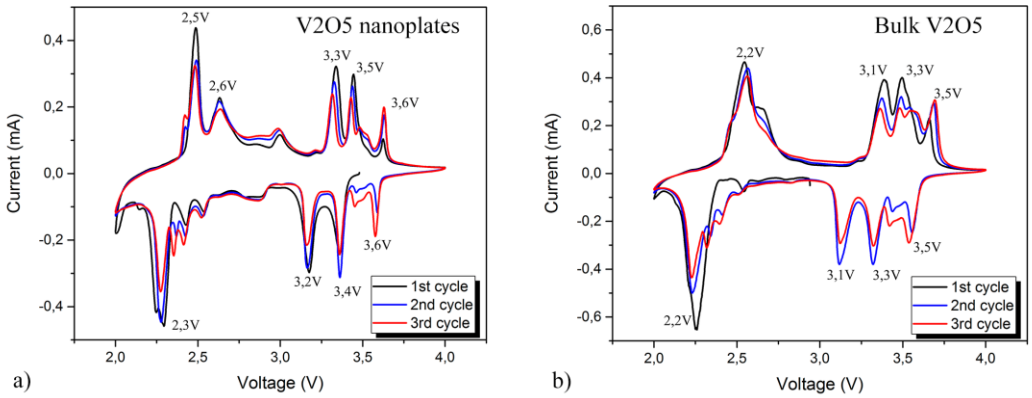

Fig. 16 – Cyclic voltammograms of a) Nanoplate V_2O_5 and b) Bulk V_2O_5 performed at a scan rate of 0.1mV s^{-1}

From the different cycles of CV on both materials, it can be found that curves have a similar shape and exhibit high peak currents, indicating similar electrochemical reaction processes are occurring. Cyclic voltammogram of Nanoplate V_2O_5 shows an anodic peak appearing at 2.6V. One possible explanation is some kind of irreversible reaction that is occurring in the transition from γ/ω. Literature suggests that these peaks disappear after some cycles [49], as can be noticed in the third cycle of Bulk V_2O_5.

Peaks in bulk V_2O_5 become weaker and broader as the cycling increases, suggesting continuous capacity fading and structure collapse after intercalation/deintercalation process [51]. The same occurs for the nanoplates, although the decrease in the peaks is lower and with an increase in the 3.6V peak, which suggests better stability during the process. The intensity is lower in the nanoplate, and although the mass loading in the two electrodes is not the same, one implication for the lower peak is a lower capacity than the bulk, contradicting what the literature says about nanoparticles.

3.3.2 Charge-discharge curves

Fig. 17 shows the 12th cycle of charge-discharge of both cathodes at a current density of 0.1C (29.4 mA h^{-1}). The 12th cycle is used to ensure that there's no irreversible reaction occurring in the cathode, that any accumulated charge in the electrodes are depleted and improve electrolyte penetration in cathodes.

Albeit the final capacities of both materials are almost identical, the curve profile is very different. Recent studies [52,53] comparing Cobalt Oxide with Manganese Oxide in potassium-ion batteries shows that smooth curves, such as with the Nanostructured V_2O_5 in this present work, are due to a deformation in the lattice when the ion is inserted, changing the relative position of the ion relatively to the oxygen. This behavior suggests that nanoplates have the capacity to distort themselves when ions are intercalated. This, though, decreases the capacity of the material but increases its stress resistance, leading to a higher number of cycles. As seen in the cyclic voltammograms, there are four pairs of redox reactions that should translate into plateaus here. There are only some slight shoulders in the curve, marked below, but they confirm the reverse-phase transformation in the discharge curve. Also, other little bumps in the discharge curve may be a related with the smaller peaks in the cathodic profile in CV. Regarding the charge curve, four little plateaus are observed corresponding to the Li^+ deintercalation process. For the bulk material, the shoulders in the discharge curve suggest that the voltage in the battery is more constant along the time.

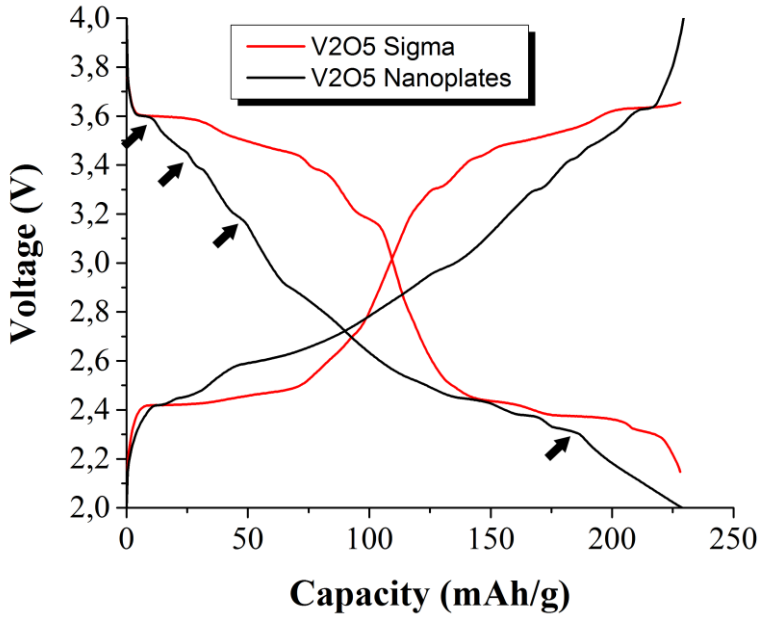

Fig. 17 – Charge-discharge curves of Nanoplate V_2O_5 and Bulk V_2O_5

3.3.3 Cycling performance

Cycling performance of both materials was studied using the galvanostatic charge-discharge test. Both cathodes were tested under a varying rate of 0.1 (29.4 mA h^{-1}), 0.2 (58.8 mA h^{-1}), 1C (294 mA h^{-1}) and again to 0.1C for the first 12 cycles and after that they were submitted to a long stress test for 100 cycles under 1C. Fig. 18 shows how the capacity varied for both cathodes for the first 12 cycles.

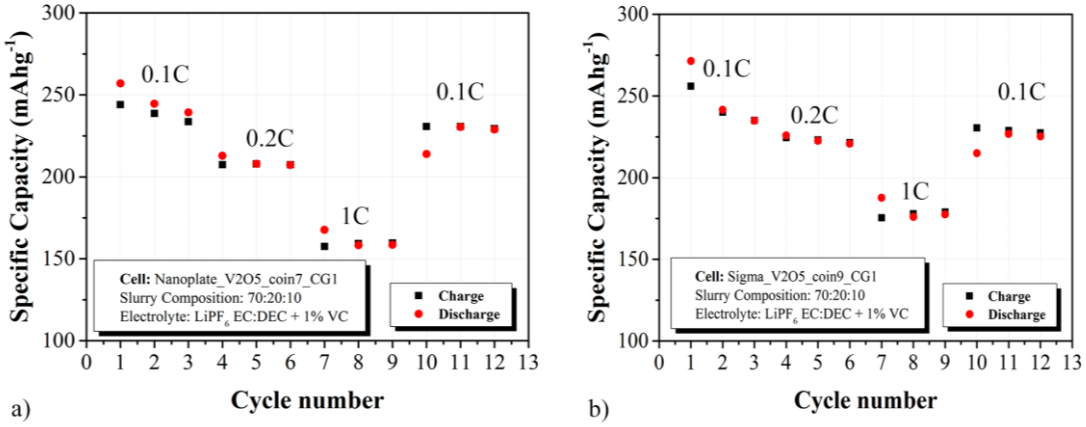

Fig. 18 – Rate performance of a) Nanoplate V_2O_5 and b) Bulk V_2O_5 for the first 12 cycles

Both cathodes showed comparable performance and capacity, although the nanostructured V_2O_5 shows lower capacity at any C-rate as expected for its lower current peak in the cyclic voltammogram. For nanostructured V_2O_5 the specific capacity varies from 230 mA h g^{-1} (0.1C) to 158 mA h g^{-1} (1C) and for bulk 231 mA h g^{-1} (0.1C) to 176 mA h g^{-1} (1C). While the maximum capacity is similar at low C-rate, an increase in the current draw (higher C-rate) shows that bulk V_2O_5 has more capacity at higher currents. One thing worth noticing is that they almost reach the theoretical capacity for Vanadium (294 mA h g^{-1}).

The coulombic efficiency (ratio between what the material can discharge over what it can charge) in early cycles is higher than 100% probably due charges present on the material prior the assembly, and after the battery stabilizes both cathodes showed 99% of coulombic efficiency.

To further evaluate the battery performance, same cathodes were subjected to 100 cycles more at 1C, to test its charge retention after long cycle life Fig. 19. When increasing the C-rate again for this test, the difference between capacities is higher than before (Δ=29 mA h g^{-1}) indicating that bulk V_2O_5 has a higher resistance to changes in current. Cathodes maintained their capacities during the cycling, with nanostructured being the most stable (92% vs 84%). Nonetheless, with the increase of cycles bulk V_2O_5 breaks, indicating a collapse in its structure causing a short-circuit in the battery.

This behavior was already expected for bulk due to the decrease of current peak in the voltammogram and, also, because the literature suggests that bulk materials have less structure resistance of with the intercalation and de-intercalation of lithium ions.

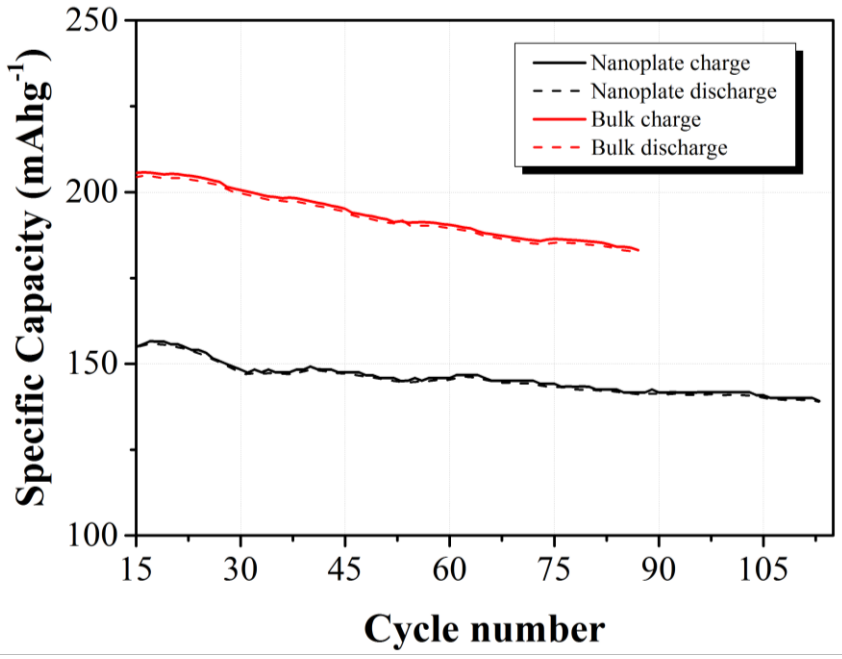

Fig. 19 - Cycling performance of bulk and nanostructured V_2O_5

4 Conclusion and Future Perspectives

A fully functional Lithium-ion battery using nanostructured V_2O_5 was successfully made in this work. Several parameters were tested, representing different morphologies on each of them. The choice of solvents represented major difference in the exfoliation process and in the aggregation of the particles. Formamide intercalated between the layers of Vanadium allowing the process of liquid exfoliation to carry on. Tip-sonication was tested in earlier phases of this thesis but produced no noteworthy results, thus, bath sonication was used and the sonication time went under test for four different times. SEM and FESEM analysis of the material showed the successful production of nanostructures, namely, nanoplates, with various thickness ranging sub-20nm to 120nm. Further studies with more solvents, as well a fine tuning of sonication parameters, such as power and frequency could lead to thinner and more uniform sheets of V_2O_5.

Formamide leads to an intermediate state of $NH_4V_3O_8$ and thermal treatment was used to evaporate $NH4^+$. TG-DSC and HT-XRD were employed to evaluate at which temperature the transition to V_2O_5 occurs (≈ 300 ºC) and further tests with XRD and XPS showed fully conversion to V_2O_5. Thermal treatment used to obtain the final product is a mere hotplate for a few seconds, so, the method of liquid-exfoliation proved to be efficient, cheap, and fast.

Several batteries were produced, using both bulk and nanostructured V_2O_5 as cathode. Two types of separators were used, Celgard and Whatman paper, but Celgard failed to produce working batteries for the Bulk V_2O_5, and for the sake of consistency it was discarded for further testing. Coin cell and T-type batteries were produced. Batteries were studied using Galvanostatic charge-discharge test and cyclic voltammetry, from there it was possible to evaluate specific capacity as well cycling stability for more than one-hundred cycles.

Recent studies regarding K-Ion Batteries indicates that the smooth curves in the charge-discharge profiles are due relaxation in the crystal lattice of layered materials, displacing the position of K^+ (in our case, Li^+) relatively to Oxygen atoms. This behavior causes a decrease in the battery capacity, but the “elastic” distortion of the lattice permits a higher resistance to intercalation and de-intercalation of ions in the material, explaining why nanostructured V_2O_5 has endured more cycles than the bulk counterpart, and also maintaining the capacity more or less constant (92% of capacity retention)

Coulombic efficiency in earlier cycles is higher than 100% due to accumulated charges in the anode, but reaching 99% as the cycles increase. This demonstrates that both materials have great charge retention. Bulk V_2O_5 had a higher potential (231 mA h^{-1} at 0.1C, 176 mA h^{-1} at 1C) than Nanostructured V_2O_5 (230 mA h^{-1} at 0.1C, 158 mA h^{-1} at 1C), and is worth nothing that according to literature this was not the initial expected result, because the decrease in size should lead to a shortened path for lithium ions, as well higher surface area, increasing the battery capacity, but as mentioned earlier, the displacement in the crystal lattice can be the reason of why the capacity is lower. Despite its higher capacity, bulk material failed before reaching one-hundred cycles, demonstrating that nanostructures possess advantages regarding battery cycling, overcoming its lower capacity.

BET analysis should be done in future work to study the porosity and the surface area of both materials used in this work, as this analysis could lead to more explanations of why the capacity of nanostructured material is lower than bulk. Post-morten morphology analysis of cathode is also interesting in the future to evaluate how the material changed during the process of intercalation and de-intercalation of Li^+.

This thesis had two major objectives, finding a way to exfoliate Vanadium Oxide was the initial goal and it was successfully achieved using the liquid-exfoliation technique. The second one was to make it meaningful, for it to have a purpose. Batteries are, today, a hot-topic in our society, and Vanadium could lead to better and cheaper batteries. The second objective was then accomplished and batteries were produced. Fine tuning the processes herein described should result in batteries capable of rivaling with LIBs.

References

1. Ma, R. & Sasaki, T. Two-Dimensional Oxide and Hydroxide Nanosheets: Controllable High-Quality Exfoliation, Molecular Assembly, and Exploration of Functionality. *Accounts Chem Res* **48,** 136–143 (2015).
2. Novoselov *et al.* A roadmap for graphene. *Nature* **490,** 192–200 (2012)
3. Huang, X., Qi, X., Boey, F. & Zhang, H. Graphene-based composites. *Chem. Soc. Rev.* **41,** 666–686 (2012).
4. Yin, H. & Tang, Z. Ultrathin two-dimensional layered metal hydroxides: an emerging platform for advanced catalysis, energy conversion and storage. *Chem. Soc. Rev.* **45,** 4873–4891 (2016).
5. Eigler, S. & Hirsch, A. Chemistry with graphene and graphene oxide-challenges for synthetic chemists. *Angew. Chem. Int. Ed. Engl.* **53,** 7720–38 (2014).
6. Kong, X., Liu, Q., Zhang, C., Peng, Z. & Chen, Q. Elemental two-dimensional nanosheets beyond graphene. *Chem Soc Rev* **46,** 2127–2157 (2017).
7. Zhang, H. Ultrathin Two-Dimensional Nanomaterials. *ACS Nano* **9,** 9451–69 (2015).
8. Geim & Novoselov. The rise of graphene. *Nature Materials* **6,** 183–191 (2007).
9. Lin, Y.-F., Hsieh, C.-T. & Wai, R.-J. Facile synthesis of graphene sheets for heat sink application. *Solid State Sciences* 22–27 (2015). doi:10.1016/j.solidstatesciences.2015.03.010
10. Coleman, J. Liquid-Phase Exfoliation of Nanotubes and Graphene. *Advanced Functional Materials* 3680–3695 (2009). doi:10.1002/adfm.200901640
11. Dines, M. Lithium intercalation via n-Butyllithium of the layered transition metal dichalcogenides. *Mater Res Bull* **10,** 287–291 (1975).
12. Zhang, Y., Zhang, L. & Zhou, C. Review of Chemical Vapor Deposition of Graphene and Related Applications. *Accounts Chem Res* **46,** 2329–2339 (2013).
13. Bernal, M. M. & Milano, D. Two-dimensional nanomaterials via liquid-phase exfoliation: synthesis, properties and applications. *Carbon Nanotechnology* **159**
14. Coleman, J. *et al.* Two-Dimensional Nanosheets Produced by Liquid Exfoliation of Layered Materials. *Science* **331,** 568–571 (2011).
15. Haber, Witko & Tokarz. Vanadium pentoxide I. Structures and properties. *Applied Catalysis A: General* **157,** 3–22 (1997).
16. Bahlawane, N. & Lenoble, D. Vanadium Oxide Compounds: Structure, Properties, and Growth from the Gas Phase. *Chemical Vapor Deposition* **20,** 299–311 (2014).
17. Bortolini, O. & Conte, V. Vanadium (V) peroxocomplexes: structure, chemistry and biological implications. *Journal of inorganic biochemistry* **99,** 1549–57 (2005).
18. Coy, H, Cabrera, R & Sepúlveda, N. Optoelectronic and all-optical multiple memory states in vanadium dioxide. *Journal of Applied …* (2010). doi:10.1063/1.3518508
19. Liao, F. *et al.* Ultrafast response flexible breath sensor based on vanadium dioxide. *J Breath Res* **11,** 036002 (2017).

20. Liu, P. *et al.* Ultrathin Nanoribbons of in Situ Carbon-Coated V3O7·H2O for High-Energy and Long-Life Li-Ion Batteries: Synthesis, Electrochemical Performance, and Charge-Discharge Behavior. *ACS Appl Mater Interfaces* **9,** 17002–17012 (2017).
21. Xu, Y. *et al.* Two-dimensional V2O5 sheet network as electrode for lithium-ion batteries. *ACS applied materials & interfaces* **6,** 20408–20413 (2014).
22. Rui, X. *et al.* Ultrathin V 2 O 5 nanosheet cathodes: realizing ultrafast reversible lithium storage. *Nanoscale* **5,** 556–560 (2012).
23. Tang, Y. *et al.* Vanadium pentoxide cathode materials for high-performance lithium-ion batteries enabled by a hierarchical nanoflower structure via an electrochemical process. *J Mater Chem* **1,** 82–88 (2012).
24. Wu, H. *et al.* One step synthesis of vanadium pentoxide sheets as cathodes for lithium ion batteries. *Electrochim Acta* **206,** 301–306 (2016).
25. Pan, A. *et al.* Facile synthesized nanorod structured vanadium pentoxide for high-rate lithium batteries. *Journal of Materials Chemistry* **20,** 9193–9199 (2010).
26. Muster *et al.* Electrical Transport Through Individual Vanadium Pentoxide Nanowires. *Adv Mater* **12,** 420–424 (2000).
27. Pan, A. *et al.* Facile synthesized nanorod structured vanadium pentoxide for high-rate lithium batteries. *J Mater Chem* **20,** 9193–9199 (2010).nhb
28. Cheng, J. *et al.* Self-assembled V 2 O 5 nanosheets /reduced graphene oxide hierarchical nanocomposite as a high-performance cathode material for lithium ion batteries. *Journal of Materials Chemistry A* **1,** 10814–10820 (2013).
29. Liang, S. *et al.* Facile synthesis of nanosheet-structured V2O5 with enhanced electrochemical performance for high energy lithium-ion batteries. *Met Mater Int* **20,** 983–988 (2014).
30. An, Q. *et al.* Supercritically exfoliated ultrathin vanadium pentoxide nanosheets with high rate capability for lithium batteries. *Physical Chemistry Chemical Physics* **15,** 16828–16833 (2013).
31. Pan, A., Wu, H., Zhang, L. & Lou, X. Uniform V2O5 nanosheet-assembled hollow microflowers with excellent lithium storage properties. *Energy & Environmental Science* **6,** 1476 (2013).
32. Liu, J. & Liu, X. Two-Dimensional Nanoarchitectures for Lithium Storage. *Advanced Materials* **24,** 4097–4111 (2012).
33. Li, Sun, Yin, Ruan & Ai. Controlling the formation of rodlike V2O5 nanocrystals on reduced graphene oxide for high-performance supercapacitors. (2013). doi:10.1021/am403739g
34. Winter, M. & Brodd, R. What Are Batteries, Fuel Cells, and Supercapacitors? *Cheminform* **35,** 4245–69 (2004).
35. Goodenough, J. B. Evolution of strategies for modern rechargeable batteries. *Acc. Chem. Res.* **46,** 1053–61 (2013).
36. Armand, M. & Tarascon, J.-M. M. Building better batteries. *Nature* **451,** 652–7 (2008).
37. Blomgren, G. The Development and Future of Lithium Ion Batteries. *Journal of The Electrochemical Society* **164,** A5019–A5025 (2016).
38. Armand. Intercalation electrodes. *Springer* 145–161 (1980).
39. Unknown. State-of-the-art of chemically grown vanadium pentoxide nanostructures with enhanced electrochemical properties.pdf.

40. Balogun, M.-S. *et al.* A review of the development of full cell lithium-ion batteries: The impact of nanostructured anode materials. *Nano Res* **9,** 2823–2851 (2016).
41. Zhang, H., Yu, X. & Braun, P. Three-dimensional bicontinuous ultrafast-charge and -discharge bulk battery electrodes. *Nature Nanotechnology* **6,** 277–281 (2011).
42. Hu, Y.-S. *et al.* Synthesis and electrode performance of nanostructured V2O5 by using a carbon tube-in-tube as a nanoreactor and an efficient mixed-conducting network. *Angewandte Chemie (International ed. in English)* **48,** 210–4 (2009).
43. Galligan, C. & Morose, G. An Investigation of Alternatives to Miniature Batteries Containing Mercury. (2004).
44. Kayyar, A., Huang, J., Samiee, M. & Luo, J. Construction and testing of coin cells of lithium ion batteries. *Journal of visualized experiments : JoVE* e4104 (2012). doi:10.3791/4104
45. Lane, R. Button cell constructions and thin profile battery constructions. *US Patent 6* (2003). at <http://www.google.com/patents/US6569564>
46. Cich. Button cell battery. (1972).
47. Nicolosi, Chhowalla, Kanatzidis, Strano & Coleman. Liquid Exfoliation of Layered Materials. *Science* **340,** 1226419–1226419 (2013).
48. Range, K.-J., Zintl, R. & Heyns, A. M. The Thermal Decomposition of Ammonium Metavanadate(V) in Open and Colsed Systems. *Z. Naturforsch* **43b,** 309–317 (1987).
49. Li, Z. *et al.* Interpenetrating network V 2 O 5 nanosheets/carbon nanotubes nanocomposite for fast lithium storage. *Rsc Adv* **4,** 46624–46630 (2014).
50. Zhang, X., Wang, J.-G., Liu, H., Liu, H. & Wei, B. Facile Synthesis of V2O5 Hollow Spheres as Advanced Cathodes for High-Performance Lithium-Ion Batteries. *Mater* **10,** 77 (2017).
51. Zhu, K. *et al.* Facile synthesis of V2O5 nanoparticles as a capable cathode for high energy lithium-ion batteries. *J Alloy Compd* **650,** 370–373 (2015).
52. Kim, H. *et al.* K-Ion Batteries Based on a P2-Type K0.6CoO2 Cathode. *Adv Energy Mater* **7,** 1700098 (2017).
53. Kim, H. *et al.* Investigation of Potassium Storage in Layered P3-Type K0.5MnO2 Cathode. *Adv Mater* **29,** 1702480 (2017).

Appendix

Fig. A. 1 - Homogeneous cathode slurry

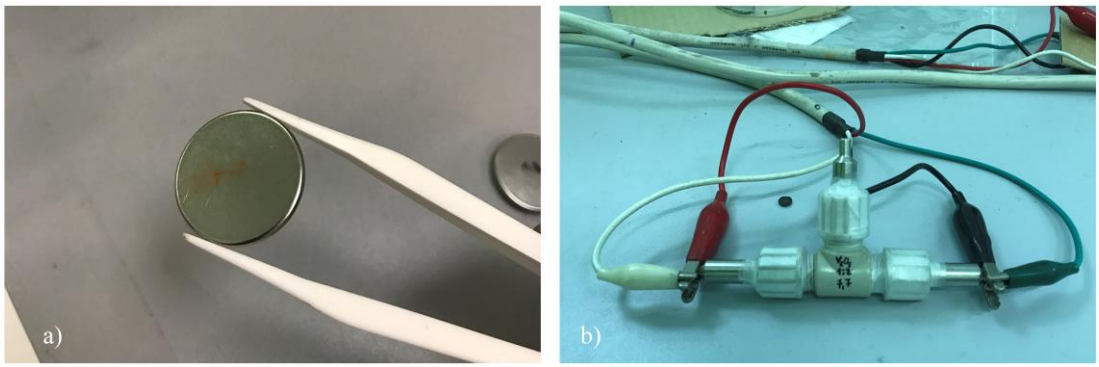

Fig. A. 2 - Examples of two batteries produced, a) coin-cell structure and b) T-cell structure

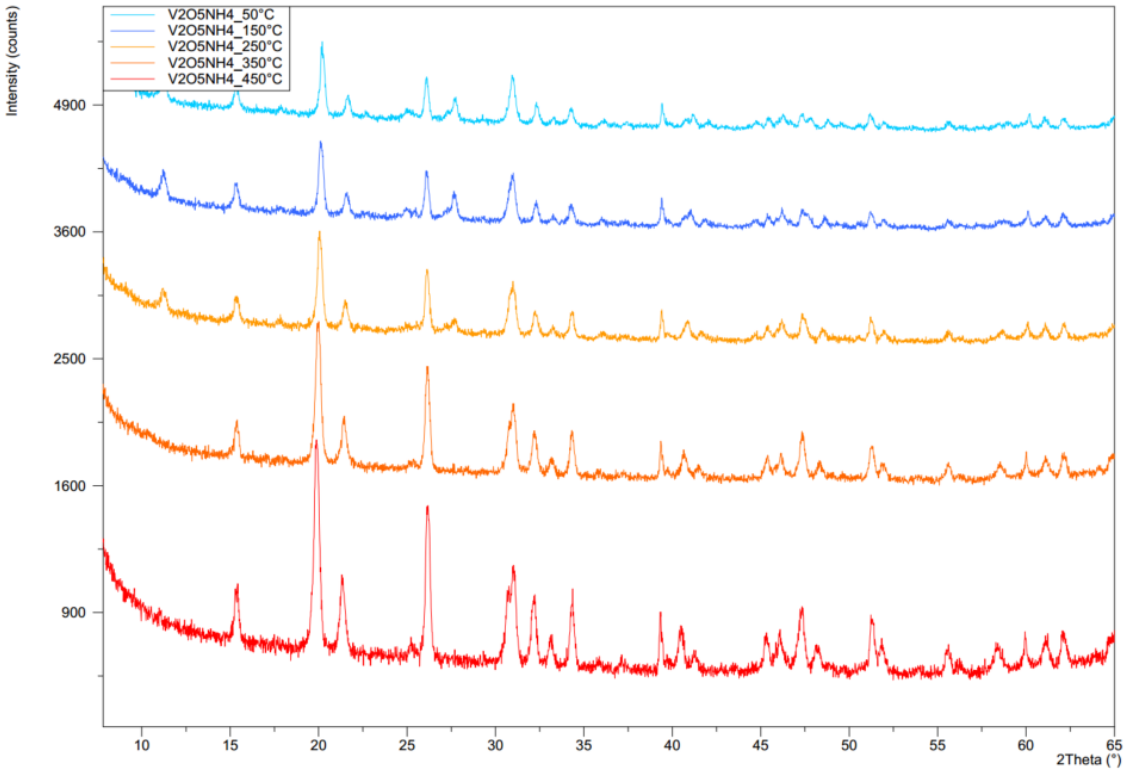

Fig. A. 3 - HT-XRD observation of material change with temperature